J Electroceram (2011) 26:78–83
DOI 10.1007/s10832-011-9631-1

Ferroelectric relaxor behavior in $Ba_{0.925}Dy_{0.075}TiO_3$ ceramic

Manas Ranjan Panigrahi · S. Panigrahi

Received: 21 October 2009 / Accepted: 24 January 2011 / Published online: 9 February 2011

Abstract Temperature and frequency dependence dielectric permittivity of $Ba_{0.925}Dy_{0.075}TiO_3$ ceramic has been studied in the temperature range of 100 K to 350 K at the frequencies, 1 Khz, 10 KHz, 100 KHz and 1 MHz for the first time. Diffuse phase transition and frequency dispersion is observed in the permittivity-vs-temperature plots. This has been attributed to the occurrence of relaxor ferroelectric behavior. The observed relaxor behavior has been quantitatively characterized based on phenomenological parameters. A comparison with the Zr doped $BaTiO_3$ has also been presented. The microstructure of as sintered samples shows a dense and almost uniform micrograph with some impurity phases, and the grains are almost spherical.

Keywords Ferroelectric · Structure · Dielectric · Relaxor

1 Introduction

Perovskite-based ferroelectrics materials attract considerable interest owing to rich diversity of their physical properties and possible applications in various technologies like memory storage devices [1], micro-electromechanical systems [2], multilayer ceramic capacitors [3], and recently in the area of opto-electronic devices [4]. These useful properties have most often been observed in lead based perovskite compounds, such as PMN, PST, PLZT [5–7]. The enhanced properties of these compounds are attributed to their relaxor behavior, observed in doped (mixed) perovskites. However these compositions have obvious disadvantages of volatility and toxicity of PbO. Therefore much effort has been carried out towards investigating environmental friendly 'Pb-free' ceramic materials. Specifically, $BaTiO_3$ and its isovalent substituted materials are the promising candidates for microwave and opto-electronic applications.

The effect of substitution on dielectric relaxation, ferroelectric phase transition and electrical properties of $BaTiO_3$ has been extensively studied [8, 9]. On partial substitution of dopants like Ca, Sr, Zr [10–12], the variation of ε around Tc gets broadened out in ceramics and single crystal samples both. Broadening increases with increasing concentration of the dopant, as also does the deviation from Curie–Weiss behavior at temperatures above the peak temperature (Tm) of the ε–T variation. The observed broadening in ε–T variation has generally been attributed to the presence of nano-regions resulting from local composition variation over length scale of 100–1,000 A°. Different nano-regions in a macroscopic sample transform at different temperatures giving rise to a range of transformation temperatures, the so-called 'Curie range'. Thus the compositional fluctuation [6, 11], in an otherwise compositionally homogenous system leads to diffuse phase transition (DPT). In compositionally homogenous systems quenched random disorder breaks the long range polar order at unit cell level, leading to broad ε–T response [7]. Such materials exhibit slow enough relaxation dynamics and hence have been termed as ferroelectric relaxors [5–7]. A series of impurity doped $BaTiO_3$ system such as Sn, Ce, Zr etc. have shown ferroelectric relaxor behavior. Among these the Zr-substituted $BaTiO_3$ ceramics have received renewed attention due to its enhanced properties both in single crystals and ceramics [12]. In the present investigation, we have studied the ferroelectric relaxor behavior in lower concentration of Dy substituted $BaTiO_3$, i.e. $Ba_{0.925}Dy_{0.075}TiO_3$ ceramics, by monitoring the

M. R. Panigrahi (✉) · S. Panigrahi
Department of Physics, National Institute of Technology, Rourkela-8, Odisha, India
e-mail: manash_123india@yahoo.co.in

variation of its dielectric permittivity with temperature in the range of 60–350 K and in the frequency range of 1 KHz to 1 MHz. Till date only limited amount of work has been carried out for Dy doping in $BaTiO_3$ [13, 14] ceramics, like its effect on dielectric and structural properties. Detailed structural and dielectric studies have been carried out. The data has been quantitatively analyzed in terms of parameters characterizing the relaxor behavior.

2 Experimental

Dysprosium modified barium titanate ceramics, with the formula $Ba_{0.925}Dy_{0.075}TiO_3$ was prepared by conventional solid-state reaction technique. High purity powders of $BaCO_3$, TiO_2 and Dy_2O_3 were hand-milled for more than 3 h with acetone in an agate mortar for homogeneous mixing of powders. High energy ball milling of homogeneous powder mixture was conducted in a planetary ball mill (Model P5, M/S Fritsch, Germany). Milling was done at room temperature in Zirconia vial (volume 250 ml) using 40 balls of 10 mm diameter made of same material. The powder mixture was milled for 2 h. The powder of the compounds was conventionally calcined at 1400°C for 4 h in an electrical furnace. Then the calcined powders were once again thoroughly mixed and ground for 2 h, mixed with 2 wt.% of PVA binder and pressed into disk-shaped pellets of 10 mm diameter and finally the green ceramics were sintered at 1450°C for 6 h. The ceramics were structurally characterized by a PANalytical X'pert-MPD X-ray diffractometer (XRD). The X-ray powder diffraction profiles of the ball milled samples were recorded using Ni-filtered Cu Kα radiation from a highly stabilized and automated Philips X-ray generator (PW 1830) operated at 30 kV and 20 mA. The generator is coupled with a Philips X-ray powder diffractometer consisting of a PW 3040 MPD controller, goniometer of radius 200 mm, and a proportional counter. For this experiment, 1° divergence slit and 1 mm receiving slit, were used. The step-scan data of step size 0.02° and step scan 0.6 s were recorded for the entire angular range 20–80°.

Scanning electron microscopy (SEM) of Jeol JSM 6480LV was used for the observation of the microstructure of the ceramics. The compositions of the element in the target were identified using energy dispersive spectrometry (EDS) attached to an SEM of Jeol JSM 6480LV. An electron beam of 10 kV and 57 μA was used for the above study. The average grain size was measured through scanning electron microscope. Dielectric measurement was carried out over frequency range 1 KHz to 1 MHz using an LCR meter (HP- Precision 4284A) connected to PC. The dielectric data was collected at an interval of 5°C while heating at a rate of 0.5°C per min.

3 Results and discussions

3.1 Structural studies

The results of X-ray diffraction characterization of the as prepared $Ba_{0.925}Dy_{0.075}TiO_3$ and $BaTiO_3$ calcined powder samples are shown in Fig. 1. The figure shows that the $Ba_{0.925}Dy_{0.075}TiO_3$ ceramic is in single tetragonal perovskite phase and the other two phases present are Dy_2TiO_5 ($2\theta=30.884°$) and Dy_2O_3 ($2\theta=60°$). Majority of the dysprosium might have gone in to the barium site and because of its small amount not that finely detectable and matches with the $BaTiO_3$ phase. The SEM micrograph of $Ba_{0.925}Dy_{0.075}TiO_3$ ceramic is shown in Fig. 2. Well shaped grains of sizes ranging from 400 to 900 nm can be seen. The theoretical and experimental wt% of [15] different elements in the sample is well comparable (i.e. the difference is less and is 5.18:4.34 for Dy).

In the higher resolution micrograph one can see that it is rich in nano contrast regions of 2–5 nm apparent sizes. The detailed features of these nano contrasts are typical to the presence of strained regions [16], not due to any secondary phase inclusions. Since these regions were found to change

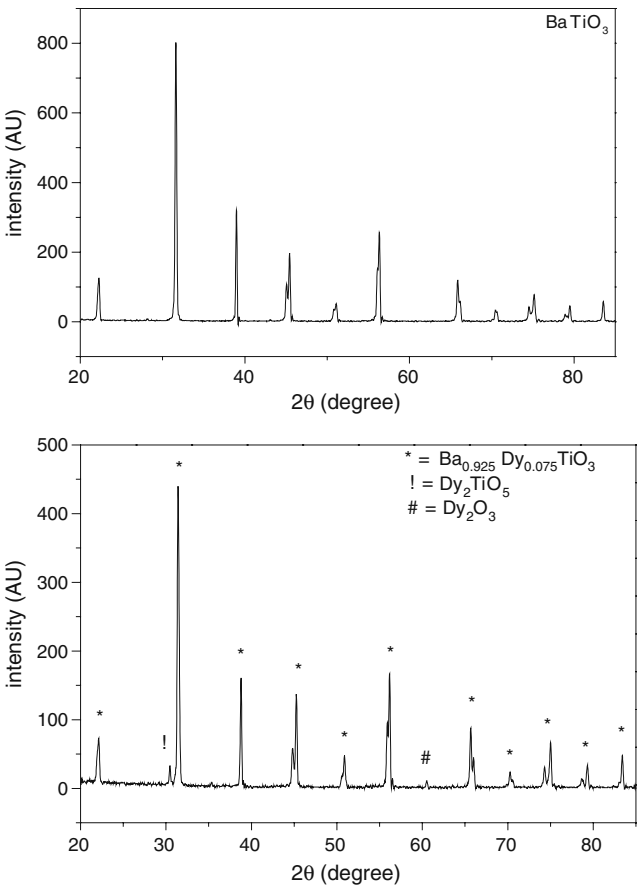

Fig. 1 XRD pattern of $BaTiO_3$ and $Ba_{0.925}Dy_{0.075}TiO_3$ ceramics showing different phases present

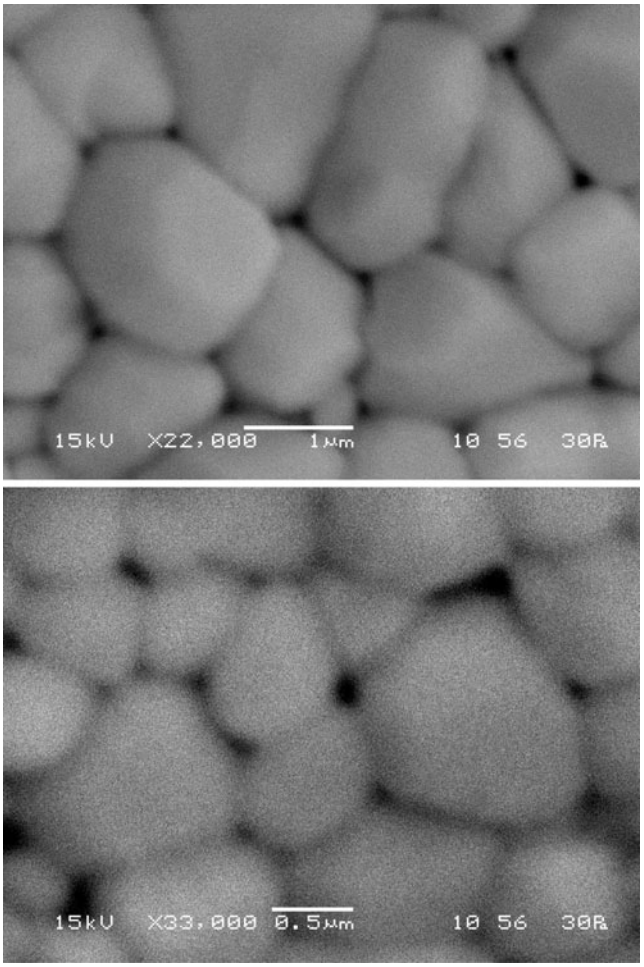

Fig. 2 SEM micrograph of $Ba_{0.925}Dy_{0.075}TiO_3$ ceramic at different resolution

contrast simultaneously during tilt, these might originate from strain fields due to some defect, like tiny dislocation loops extending just to few lattice sites with their burger vectors parallel. The occurrence of these defect features in $Ba_{0.925}Dy_{0.075}TiO_3$ will lower its structural correlation length as compared to $BaTiO_3$ in which no such features were found. The 'structural correlation length' is basically a measure of the effective extent to which the long range order of an atomic arrangement gets limited as a result of the cumulative effect of all types of defect features, which somehow either interrupt the chemical order or produce strain in the lattice. Beyond this extent the atoms don't scatter coherently and contribute to the width of the diffraction maxima. Thus the structural correlation length may be used as a measure of comparison of defects presence in two similar types of structures. Thus to compare the presence of defects in the bulk samples of $Ba_{0.925}Dy_{0.075}TiO_3$ and $BaTiO_3$, structural correlation lengths were calculated from the half-widths of the first sharp diffraction peak (FSDP), after applying instrumental broadening and $K\alpha_2$ corrections. These were found to be ~33 A° and ~26 A° respectively for $Ba_{0.925}Dy_{0.075}TiO_3$ and $BaTiO_3$. The interlayer separation with an effective periodicity, R (the atom–void distance [17]), was found to be 2.04 A° and 3.10 A° for $Ba_{0.925}Dy_{0.075}TiO_3$ and $BaTiO_3$ ceramics respectively for FSDP. It should be noted that the size of even the smallest grain, as seen through SEM, is at least an order of magnitude larger than the structural correlation length. A flavour to the FSDP related parameters in terms of structural correlation length and effective periodicity is explained below.

The FSDP parameters such as the interlayer separation, quasi periodic in nature with an effective periodicity (R) and correlation length (L), over which such periodicity is maintained, of atomic density fluctuations, regardless of the precise atomic origin of such fluctuations are calculated using the general expressions [18],

$$R = \frac{2\pi}{S} \tag{1}$$

where S is the magnitude of the scattering vector and is given by

$$S = \frac{4\pi \sin\theta}{\lambda} \tag{2}$$

corresponds to the position of the FSDP, and

$$L = \frac{2\pi}{\beta} \tag{3}$$

where β is the full width at half maximum (FWHM) of the FSDP.

3.2 Dielectric studies

The temperature dependence of the dielectric permittivity of $Ba_{0.925}Dy_{0.075}TiO_3$ ceramic are shown in Fig. 3. Unlike $BaTiO_3$ the transition is quite diffuse. The paraelectric to ferroelectric phase transition temperature (Tc) as compared to that of the BaTiO3, have decreased. The three phase transitions which are observed in $BaTiO_3$ have got pinched and merged into one round peak in ε–T variation. The results obtained can be described as in the following:

(1) There is a broad peak around Tm = 150 K in the ε–T curve. With increasing frequency Tm increases, while the magnitude of the peak decreases.
(2) There is a strong dielectric dispersion in radio frequency region around and below Tm in the ε–T curve.

The above described features of (ε–T) variations shown in Fig. 3 are very much similar to the observations by Cross, Lu, Cheng, Chen and other workers [5, 6, 10, 12,

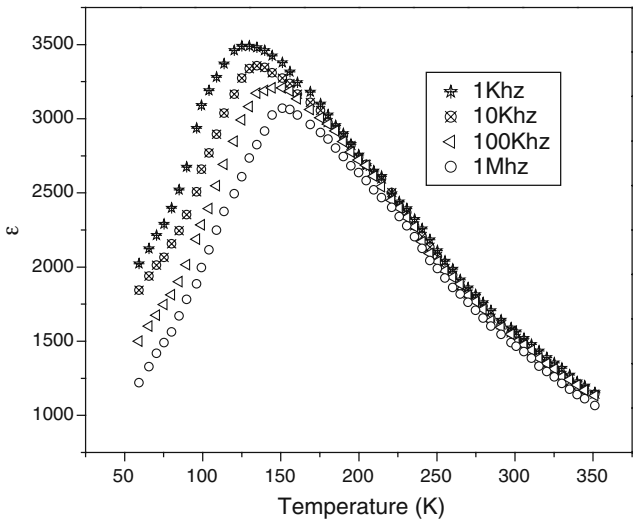

Fig. 3 Relative permittivity Vs. temperature curve at different frequencies

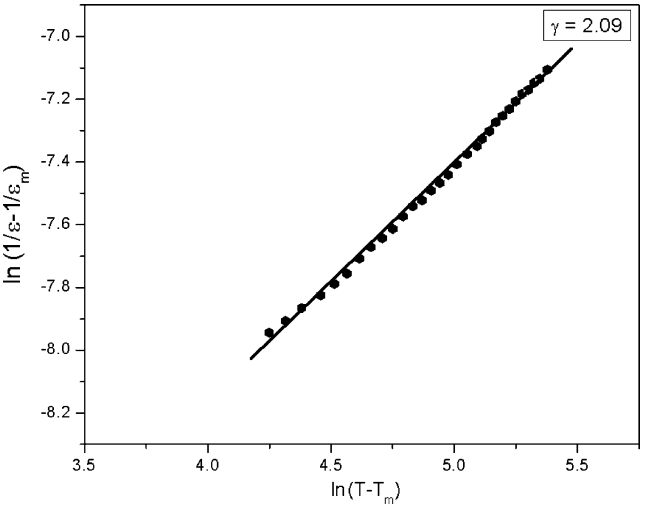

Fig. 5 The plot of $\ln(1/\varepsilon - 1/\varepsilon_m)$ as a function of $\ln(T-T_m)$

16] for various lead based and lead free ferroelectric relaxor materials. In order to further confirm the relaxor behavior, the quantitative characterizations as described in the following have been done.

3.3 Permittivity variation in the high temperature side

It is known that dielectric permittivity of a normal ferroelectric above Curie temperature follows the Curie–Weiss law described by

$$\varepsilon = \frac{C}{(T - T_0)} (\mathrm{T} > \mathrm{T_C}), \tag{4}$$

where T_0 is the Curie–Weiss temperature and C is the Curie–Weiss constant.

Figure 4 shows the inverse of ε as a function of temperature at 10 Khz and its fit to the experimental data by Curie–Weiss law. A deviation from Curie–Weiss law can be clearly seen. The parameter ΔTm, which is often used to show the degree of deviation from the Curie–Weiss law is defined as

$$\Delta T_m = T_{CW} - T_m. \tag{5}$$

where T_{cw} denotes the temperature from which the permittivity starts to deviate from the Curie–Weiss law and T_m represents the temperature of the dielectric maximum. The T_{CW} as determined from the Curie–Weiss fit, is T_{CW} = 144 K, and ΔTm is thus found to be = 12 K at 10 KHz. For such relaxor behavior a modified Curie–Weiss law has been proposed by Uchino and Nomura [19], to

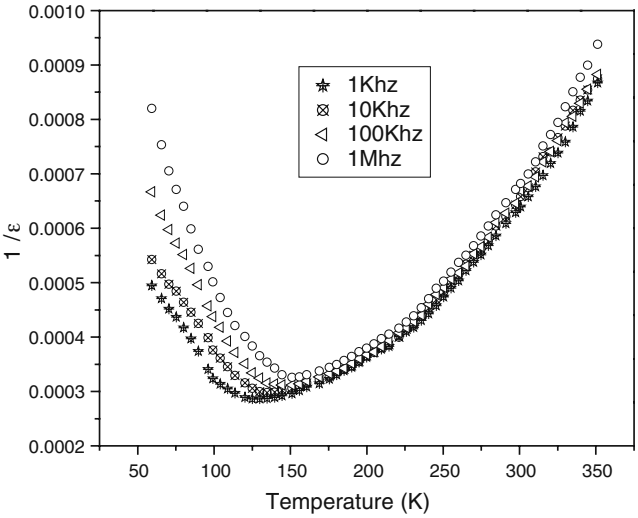

Fig. 4 Inverse Relative permittivity Vs. temperature curve at different frequencies

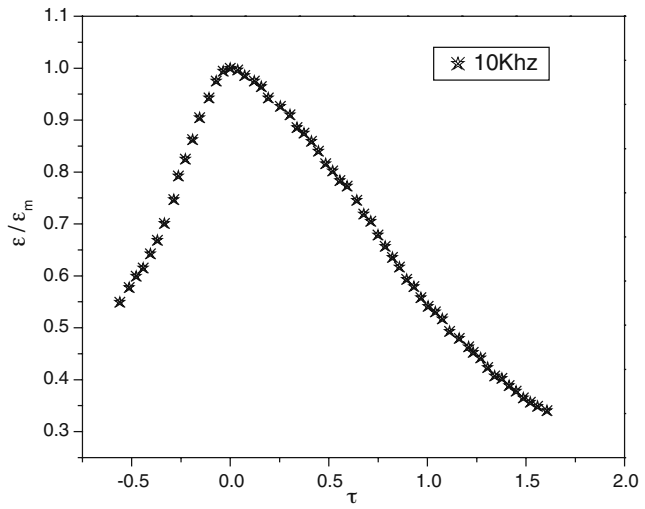

Fig. 6 The plot of reduced dielectric constant ($\frac{\varepsilon}{\varepsilon_m}$) as a function of reduced temperature (τ) at different frequencies

describe the diffuseness of the phase transition. This is defined as in the following.

$$\frac{1}{\varepsilon} - \frac{1}{\varepsilon_m} = (T - T_m)^{\gamma}/C \quad (6)$$

where γ and C are assumed to be constant. The parameter γ gives information on the character of the phase transition. Its limiting values are $\gamma = 1$ and $\gamma = 2$ in expression (6) of the Curie–Weiss law, $\gamma = 1$ is for the case of a normal ferroelectric and the quadratic dependence is valid for an ideal ferroelectric relaxor respectively [12, 20]. Thus the value of γ can also characterize the relaxor behavior. The plot of $\ln(1/\varepsilon - 1/\varepsilon_m)$ as a function of $\ln(T - T_m)$ is shown in the Fig. 5 by fitting with Eq. 6, the exponent γ, determining the degree of the diffuseness of the phase transition, is obtained from the slope of $\ln(1/\varepsilon - 1/\varepsilon_m)$ versus $\ln(T - T_m)$ plot. We obtained the value of the parameter γ to be 2.09, which is very close to 2, suggesting that the prepared ceramic is a relaxor ferroelectric [18, 19]. Yet another parameter, which is used to characterize the degree of relaxation behavior in the frequency range of 100 Hz to 100 KHz, is described [20] as

$$\Delta T_{\mathrm{Re}lax} = T\varepsilon_m(100KHz) - T\varepsilon_m(1KHz) \quad (7)$$

The value of ΔTrelax was determined to be 14 K for the present sample. The above characterization done on the basis of Curie–Weiss law and the value of empirical parameters like ΔTm, γ, and ΔTrelax suggest that the permittivity of $Ba_{0.925}Dy_{0.075}TiO_3$ ceramic follows Curie–Weiss law only at temperatures much higher than Tm. Thus the large deviation from the Curie–Weiss behavior, large relaxation temperature γ Trelax, and γ=2.09, suggests that $Ba_{0.925}Dy_{0.075}TiO_3$ is a relaxor ferroelectric.

The broadening of the phase transition is better illustrated by plotting the reduced dielectric constant ($\frac{\varepsilon}{\varepsilon_m}$) as a function of reduced temperature (τ) at different frequencies (Fig. 6). Reduced temperature (τ) is defined as $\frac{(T-T_m)}{T_m}$. The full width of the plot has very little dispersion over a wide frequency range similar to the observation made in other relaxor materials [21].

The occurance of relaxor in Zr substituted barium titanate [12, 22, 23] has been attributed to the existence of nano-polar region due to Zr doping. The replacement of Ti^{4+} by Zr^{4+} ions is known in the classical ferroelectric [22, 23]. The increasing substitution decreases the Curie temperature. The probable reason may be the presence of secondary phases in small amount and may be attributing to the compositional heterogeneity defect. As it is seen that, rare earth may substitute A-site or B-site or results in the evolution of new peaks or secondary phases.

It can be seen from the comparative structural study of $Ba_{0.925}Dy_{0.075}TiO_3$ and $BaTiO_3$ using XRD and SEM, that nano scale defect features are present in $Ba_{0.925}Dy_{0.075}TiO_3$. It appears that substitution of Dy causing nano-scale compositional heterogeneity due to presence of defects [21–24] creating nano polar domains. It has been suggested that polar nano-domains are responsible for the relaxational behavior in PMN and PLZT [10] systems. The substitution of Dy ions tends to make the distance between off center Ti dipoles larger and thus weakening the correlation between these dipoles. The mismatch in the size of Ti and Dy ions will cause substitutional distortion of the oxygen octahedra, giving rise to the local electric-field and strain-field. Also the ferroelectric behavior of $Ba_{0.925}Dy_{0.075}TiO_3$ depends on the competitions between long-range ordering owing to strong correlation of the off center Ti dipoles and the random fields induced by Dy doping, thus the existence of these fields leads to the destruction of long-range ferroelectric ordering and nanopolar coherent domains get formed giving rise to the relaxor behavior.

4 Conclusions

Based on the X-ray diffraction and dielectric studies of $Ba_{0.925}Dy_{0.075}TiO_3$ ceramic it can be concluded that Dy substitution in $BaTiO_3$ forms a perovskite tetragonal phase structure at room temperature. The occurrence of diffuse phase-transition and strong frequency dispersion of maxima in the permittivity versus temperature, strongly indicate the relaxor behavior for this $Ba_{0.925}Dy_{0.075}TiO_3$ ceramic. The quantitative characterization and comparison of the relaxor behavior based on empirical parameters (ΔTm, γ, and ΔT_{relax}) confirms its relaxor behavior.

References

1. A.I. Kingon, S.K. Streiffier, C. Basceri, S.R. Summerfelt, MRS Bull. **21**, 46 (1996)
2. D.L. Polla, L.F. Francis, MRS Bull. **21**, 59 (1996)
3. Y. Sakabe, T. Takagi, K. Wakino, D.M. Smith, in *Advances in Ceramics, Vol. 19*, ed. by J.B. Blum, W.R. Cannon (Am. Ceram. Soc. Inc., Ohio, 1986), p. 103
4. F.J. Walker, A. McKee, Nanostruct. Mater. **7**, 221 (1996)
5. Z.G. Lu, G. Calvarin, Phys. Rev. B **51**, 2694 (1995)
6. L.E. Cross, Ferroelectric **76**, 241 (1987)
7. N. Settler, L.E. Cross, J. Appl. Phys. **51**(8), (1980).
8. M. Maglione, M. Belkaoumi, Phys. Rev. B **45**, 2029 (1992)
9. J.N. Lin, B. Wu, J. Appl. Phys. **68**, 985 (1990)
10. P. Victor, R. Ranjith, S.B. Krupanidhi, J. Appl. Phys. **12**, 7702 (1994)
11. V.S. Tiwari, N. Singh, D. Pandey, J. Phys. Condens. Matter **7**, 1441 (1995)
12. Z. Yu, C. Ang, R. Guo, A.S. Bhalla, J. Appl. Phys. **92**, 2655 (2002)
13. W.H. Payne, V.J. Tennery, J. Am. Ceram. Soc. **48**, 413 (1965)
14. V. Tura, L. Mitoseriu, Europhys. Lett. **50**(6), 810 (2000)
15. M.R. Panigrahi, S. Panigrahi, Phys. B **404**, 4267 (2009)

16. P.B. Hirsch, A. Howie, R.B. Nicholson, D.W. Pashley, J. Whelan, *Electron microscopy of thin crystals* (Butterworths, London, 1969), pp. 327–337
17. S.R. Elliott, Phys. Rev. Lett. **67**, 711–714 (1991)
18. S.R. Elliott, J Non-Cryst Solids **182**, 40–48 (1995)
19. K. Uchino, S. Nomura, Integr. Ferroelectr. **44**, 55 (1982)
20. C. Ang, Z. Jing, Z. Yu, J. Phys. Condens. Matter **14**, 8901 (2002)
21. M. Tyunina, J. Levoska, A. Sternberg, S. Leppavuori, J. Appl. Phys. **86**, 5179 (1999)
22. J. Ravez, M. Pouchard, P. Hagenmuller, Eur. J. Solid State Inorg. Chem. **28**, 1107 (1991)
23. J. Ravez, A. Simon, Solid State Sci. **2**, 525–529 (2000)
24. J. Ravez, A. Simon, Eur. J. Solid State Inorg. Chem. **37**, 1199 (1997)